Cancer Cell, Volume *13*

Supplemental Data

AID-Dependent Activation of a *MYC* Transgene Induces Multiple Myeloma in a Conditional Mouse Model of Postgerminal Center Malignancies

Marta Chesi, Davide F. Robbiani, Michael Sebag, Wee Joo Chng, Maurizio Affer, Rodger Tiedemann, Riccardo Valdez, Stephen E. Palmer, Stephanie S. Haas, A. Keith Stewart, Rafael Fonseca, Richard Kremer, Giorgio Cattoretti, and P. Leif Bergsagel

Supplemental Experimental Procedures

Construct generation:

The following DNA fragments were assembled by classical molecular cloning techniques into a pCDNA3.1 vector (Invitrogen) gutted of its CMV promoter:
1) The Vk21E region was amplified from genomic tail DNA of a C57BL/6 mouse by combined PCR of products generated by primers o679-o690 and o689-o676 in which the two ATGs in the leader exon were mutated to ACG (in red) to abrogate initiation of translation from these sites.
2) The Kozak consensus motif with initiation of translation ATG (in green) and the premature STOP codon (in red) were introduced with primer o448 (see below).
3) The complete Jk5 intron was PCR-amplified from pBR322 plasmid with an EcoRI-BamHI fragment including mouse Jkappa through Ckappa (gift from Dr. Edward Max) with primers o448-o423 and o424-o425.
4) The portion of human *MYC* gene derived from pSV2neo plasmid containing exons 1, 2, and 3 (gift from Dr. Jim Battey), whereby the o426-o427 PCR product (with portion of exon 2) was combined to a 3.4kb Kas-EcoRI fragment (including portion of exon 2, intron 2, exon 3 and polyA tail).
5) The 1.3kb XhoI fragment with 3'kE originated from pBKS plasmid containing 20.8.3JV-Ck (gift from Dr. Mark Shlomchik).
Cloned PCR products were sequenced and verified by comparing with the NCBI database. The construct was finally excised from the plasmid backbone with MluI and NotI and microinjected into C57BL/6 fertilized eggs (MSKCC Mouse Genetics Core,New York).

o423	5-ACCATGACTTTTGCTGGCTGTAG-3
o424	5-GGGCATAAACTGCTTTATCCAGTG-3
o425	5-GGTGAAGCTAACGTTGAGGGGCTGAGGAAGGAAGCACAGAGGATGG-3
o426	5-CCATCCTCTGTGCTTCCTTCCTCAGCCCCTCAACGTTAGCTTCACC-3
o427	5-AAGGGAGAAGGGTGTGACCGCAAC-3
o448	5-GGATCCATGGGATAGTACCCTTATGATGTGCCAGATTATGCCAAGGTA AGTACACTTTTCTCATCT-3
o676	5-GTACTATCCCATGGTGGCGGATCCTACAGCTAAGGAAGCAGG-3

o679	5-ACGCGTAAAAATGTATGACCCTTGGCATGGA-3
o689	5-GCTCTCAGAGACGGAGACAGACACACTCCTGTTACGGGTACTGCTG-3
o690	5-CAGCAGTACCCGTAACAGGAGTGTGTCTGTCTCCGTCTCTGAGAGC-3

Southern blot:

10µg genomic DNA, extracted by salting out procedure, were digested with HindIII and separated on a 0.6% gel as previously described(Chesi et al., 1997). As a probe, the exact 1.3kb XhoI fragment containing the mouse 3'kE that was cloned in the transgenic vector was labelled by nick-translation. Transgene copy number was estimated by densitometric analysis of a phosphor imager (Storm, GE Healthcare) scanned image using the ImageQuant software (Molecular Dynamics). Briefly, the integrated density of all the pixels in the area of each band was quantified and adjusted by a background subtraction of density in an adjacent blank area of the same size. Then, the pixel density of the transgenic band for each line was divided by the density value of the corresponding germline band, and the resulting number was multiplied by two, since there are two copies (two alleles) in the germline band.

293-T transfection and Western blot:

Cells were transfected with 10µg of plasmid by calcium phosphate. Whole cell extracts were prepared 48 hours post transfection in RIPA buffer. 35µg of protein were separated by SDS-PAGE, blotted on nitrocellulose and probed with anti human MYC (9E10 Covance) or with beta-actin (AC-15 Sigma).

LPS stimulation and multi tissue Northern blot:

6-8 weeks old mice were euthanized and single cell suspensions of splenocytes were generated by dissociation of a full spleen by repetitive mincing between frosted slides. After red cells lysis in ACK buffer, splenocytes were plated at $5x10^5$/ml in RPMI/10%FCS the presence of 12.5mg/ml LPS serotype B5 (Sigma) and growth for 5 days. Flow cytometry on LPS stimulated cells demonstrated 30% $CD138^+$ cells. Other tissues were collected from 6-8 weeks old mice and pulverized in liquid nitrogen using mortar and pestle. BM cells were collected by flushing out ilium, femur, tibia, humerus and radius with PBS. On average, >100 million BM nucleated cells were obtained from each mouse. RNA was isolated using Trizol (Invitrogen). Northern blot was performed as described(Chesi et al., 1997). Human MYC probe containing exons 2 and 3 was amplified by RT-PCR from a human myeloma cell line using primers 5'-AACAGGAACTATGACCTCGACTAC and 5'-CTTTTCCTTACGCACAAGAGTTCC.

SPEP.

Mice were bled at ten-week interval by tail grazing. Blood was collected into Microtainer tubes (Becton Dickinson) and spun for 10 minutes at 2,300g. Sera were diluted 1:2 in barbital buffer (Beckman Coulter) and analyzed on a Paragon apparatus (Beckman Coulter) according to manufacturer's instruction. 1% agarose (Seakem HE, Cambrex) gels in barbital buffer were polymerized onto Gel Bond films (Cambrex) placed in between minigel casting plates (Biorad).

Immuno-histochemistry:

4mm sections from formalin fixed, paraffin embedded and decalcified (for bone tissues only) tissue blocks were deparaffinized in xylene and boiled in 1mM EDTA pH=8 prior staining with the following primary antibodies: rabbit anti-MYC (sc-764_N-262), goat anti-Ki67 (sc-7846_M-19, all from Santa Cruz), rat anti-CD138 (281-2) and B220 (RA3-6B2) (both from BD Pharmingen). For double stainings, primary antibodies were first counterstained with alkaline phospatase-conjugated (first staining) or HRP-conjugated (second staining) secondary isotype-specific antibodies (Jackson Immunoresearch), then developed with NBT-BCIP (Roche), and DAB (Dako) or AEC (AminoethylCarbazole, Sigma) as previously published(Cattoretti et al., 2006).

Mutational analysis:

$CD138^+$ PCs were magnetically purified on MACS MS columns (Miltenyi Biotec). Spleen and tumor DNAs were extracted by direct salting out or from Trizol lysates (Invitrogen). cDNA from purified plasma cells was generated from Trizol extracted RNA using Superscript-III reverse transcriptase (Invitrogen). VDJ fragments were first PCR amplified from DNA or cDNA with a proof-reading enzyme (pfu-ultra, Stratagene) using equimolar amounts of sense VH-FR1 degenerated primers(Wang et al., 2000) and four antisense JH specific primers(Delassus et al., 1995), then were directly sequenced or subcloned into pCR4Blunt-TOPO vector (Invitrogen) before sequencing single colonies. Results were confirmed by direct sequencing of independent RT-PCR reactions using a forward primer that anneals to the framework region III of the most abundantly used VH J558 family(Cattoretti et al., 2005), and a reverse primer annealing to the first coding exon of all four Cgamma (AAGTAGCCCTTGACCAGGCATCC). The obtained sequences were compared to the germline mouse VH database, containing sequences of the entire VH locus in C57BL/6, using the IgBLAST software (http://www.ncbi.nlm.nih.gov/igblast/). For mutational analysis at the transgenic locus, the region surrounding the engineered stop codon was first amplified with pfu-ultra from spleen, tumor, or purified PC DNA or cDNA, using a forward primer downstream the VK promoter (5'-CCTAATAAGCATCCTCTCTTCCAG) and reverse primers in exon 3 of MYC (5'-CCTTTTGCCAGGAGCCTG). PCR fragments were subcloned into pCR4Blunt-TOPO vector and single colony sequencing was performed.

Light chain RT-PCR:

RT-PCR was performed on BM mononuclear cells from non-immunized and NP-immunized Vk*MYC mice by 20 round of amplification using Ig Jλ and Cλ consensus primers: 5'-GTGGAACCAAAGTSACTGTCCTAG and 5'-GACARACTCTTCTCCACAGTGT.

Hemoglobin:

Hgb levels from peripheral blood were measured on a Coulter Analyzer instrument (Beckman Coulter) and compared using the Mann Whitney test.

ELISA:

Mouse sera were diluted at 1:10,000 – 1:400,000 and total Ig concentration was determined using Ig subtype specific ELISAs quantitation kits (Bethyl Laboratories). Ig levels were compared using the Mann Whitney test.

Bone analysis:

Dual-energy X-ray absorptiometry (DEXA) analysis was performed on age (approximately 70wks) and sex matched wild type and Vk*MYC mice. Femoral head BMD was measured using a PIXIMUS bone densitometer (PIXIMUS, GE Medical Systems). A phantom (PIXIMUS) was used to calibrate the densitometer before each experiment. For micro-CT of bone samples, femurs of age (70wks) and sex matched wild type and VK*MYC mice were fixed in 10% formalin, scanned by micro-CT at x40 magnification with a SkyScan 1072, and analyzed with bone analysis software (v. 2.2f; Skyscan, Aartselarr, Belgium). During scanning, the samples were enclosed in a tightly fitting, rigid plastic tube to prevent movement. Analyses of the trabecular bone were carried out in a 2.3-mm-thick region of the tibia, distal to the growth plate of the knee joint. The software was used to separate regions of trabecular bone from cortical bone in the sections. Thresholding was then applied to the images to segment the bone from the background, and the same threshold setting was used for all the samples.

Transplant:

10-20 million femoral BM nucleated cells from Vk*MYC donor mice were resuspended in 100µl PBS and transplanted by intra-cardiac injection into 8-14 week old WT C57BL/6 recipient mice, lethally irradiated with 10 Gy.

Drug studies.

Vk*MYC mice with significant gammopathy (>20g/l on SPEP) were selected for drug treatment (5 mice per treatment arm). Dexamethasone (1mg/kg IP) and melphalan (2.5mg/kg IP) were given once a day for 5 days at previously published doses that approximate use in the clinic(Tassone et al., 2005). Bortezomib (0.5mg/kg IP twice a week for 4 weeks) was administered over a longer period of time to approximate one cycle of treatment(LeBlanc et al., 2002). Fludarabine (34mg/kg IP x5 days) and vincristine (0.5mg/kg IP once) doses were chosen based on previous publications and the reported maximally tolerated dose respectively(Johnson et al., 2006; Liem et al., 2004). Hydroxyurea (100mg/kg IP twice a day for 5 days) was given at a dose which was limited by myelotoxicity(Van den Berg et al., 1994). Myelotoxicity in all mice was measured by weakly complete blood counts while outcome was measured by weekly SPEP.

Antigen-specific immunoblotting (Eastern blot):

NP-BSA-impregnated PVDF filters, Hybond-P (Amersham Biosciences), were prepared as described(Nooij et al., 1990). Briefly, filters were incubated in 100µg/ml NP-BSA (Biosearch Technologies) in 0.5 M $NaHCO_3$, rinsed in PBS/0.05% Tween 20 (PBS/T), blocked in 1% BSA, fixed in 2.5% gluteraldehyde in 0.2M Na-acetate (pH 5.0) and finally rinsed in PBS/T. SPEP gels were blotted onto the NP-membranes by capillarity. After blocking in 5% low fat milk in PBS/T, the membranes were incubated with alkaline phosphatase goat anti-mouse IgG (ICN Biochemicals) in PBS/T, washed and developed using a NBT/BCIP (Sigma).

Gene-set Enrichment Analysis.

GSEA has been described elsewhere(Subramanian et al., 2005). Briefly, the method requires two inputs: (1) a list of genes (*L*) ranked based on the correlation between their expression and the class distinction by using a suitable metric and (2) *a priori* defined gene sets (*S*) (e.g pathways or promoter motif sequences extracted from published experimental data or curated databases). The

goal of GSEA is to determine whether the members of *S* are randomly distributed throughout *L* or primarily found at the top or bottom, in which case the gene set is correlated with the phenotypic class distinction (in our case MM or MGUS). The ranking metric used was Signal2Noise, and the phenotype was permutated with 1000 permutations to estimate the statistical significance (*p*-value) and false discovery rate (FDR) of enrichment (*q*-value).

Gene expression analysis.

Probe level intensity was generated using MAS5.0. Experiments from the same platforms are grouped and analyzed together. Data is median centered and analyzed in Genespring GX 7.3.1. *MYC* expression is derived from information related to probe-set 202431_s_at. A proliferation index is calculated based on the median expression of 7 genes (*TYMS* – 202589_at, *KIAA0101* – 202503_s_at, *CKS1B* – 201897_s_at, *TOP2A* – 201292_at, *CCNB1* – 214710_s_at, *UBE2C* – 202954_at, *TRIP13* – 204033_at)(Bergsagel et al., 2005).

MYC signature and Index.

We used genes recently identified as 'first neighbor' to *MYC* in a MYC sub-network and validated as DNA binding target gene of *MYC* by chromatin immuno-precipitation to form the MYC signature. These genes are: *POLD2, PPAT, SRM, ZNF593, JTVI, EEF1E1, TRAP1, NME1, PAICS, EIF3S9, BOP1, EBNA1BP2, NOL5A, BYSL, MRPL12, RPL42, TCP1, ATIC, ZRF1, HRMT1L3*(Basso et al., 2005). The MYC index is calculated as the median expression of these genes.

Statistical Analysis.

MYC expression and MYC index is compared between MM and MGUS using the student's t-test. 2-tailed *p*-values are reported and *p*-value less than 0.05 is considered significant.

Supplemental References

Basso, K., Margolin, A. A., Stolovitzky, G., Klein, U., Dalla-Favera, R., and Califano, A. (2005). Reverse engineering of regulatory networks in human B cells. Nat Genet *37*, 382-390.

Bergsagel, P. L., Kuehl, W. M., Zhan, F., Sawyer, J., Barlogie, B., and Shaughnessy, J., Jr. (2005). Cyclin D dysregulation: an early and unifying pathogenic event in multiple myeloma. Blood *106*, 296-303.

Cattoretti, G., Pasqualucci, L., Ballon, G., Tam, W., Nandula, S. V., Shen, Q., Mo, T., Murty, V. V., and Dalla-Favera, R. (2005). Deregulated BCL6 expression recapitulates the pathogenesis of human diffuse large B cell lymphomas in mice. Cancer Cell *7*, 445-455.

Cattoretti, G., Buttner, M., Shaknovich, R., Kremmer, E., Alobeid, B., and Niedobitek, G. (2006). Nuclear and cytoplasmic AID in extrafollicular and germinal center B cells. Blood *107*, 3967-3975.

Chesi, M., Nardini, E., Brents, L. A., Schrock, E., Ried, T., Kuehl, W. M., and Bergsagel, P. L. (1997). Frequent translocation t(4;14)(p16.3;q32.3) in multiple myeloma is associated with

increased expression and activating mutations of fibroblast growth factor receptor 3. Nat Genet *16*, 260-264.

Delassus, S., Gey, A., Darche, S., Cumano, A., Roth, C., and Kourilsky, P. (1995). PCR-based analysis of the murine immunoglobulin heavy-chain repertoire. J Immunol Methods *184*, 219-229.

Johnson, A. J., Lucas, D. M., Muthusamy, N., Smith, L. L., Edwards, R. B., De Lay, M. D., Croce, C. M., Grever, M. R., and Byrd, J. C. (2006). Characterization of the TCL-1 transgenic mouse as a preclinical drug development tool for human chronic lymphocytic leukemia. Blood *108*, 1334-1338.

LeBlanc, R., Catley, L. P., Hideshima, T., Lentzsch, S., Mitsiades, C. S., Mitsiades, N., Neuberg, D., Goloubeva, O., Pien, C. S., Adams, J.*, et al.* (2002). Proteasome inhibitor PS-341 inhibits human myeloma cell growth in vivo and prolongs survival in a murine model. Cancer Res *62*, 4996-5000.

Liem, N. L., Papa, R. A., Milross, C. G., Schmid, M. A., Tajbakhsh, M., Choi, S., Ramirez, C. D., Rice, A. M., Haber, M., Norris, M. D.*, et al.* (2004). Characterization of childhood acute lymphoblastic leukemia xenograft models for the preclinical evaluation of new therapies. Blood *103*, 3905-3914.

Nooij, F. J., Van der Sluijs-Gelling, A. J., Jol-Van der Zijde, C. M., Van Tol, M. J., Haas, H., and Radl, J. (1990). Immunoblotting techniques for the detection of low level homogeneous immunoglobulin components in serum. J Immunol Methods *134*, 273-281.

Subramanian, A., Tamayo, P., Mootha, V. K., Mukherjee, S., Ebert, B. L., Gillette, M. A., Paulovich, A., Pomeroy, S. L., Golub, T. R., Lander, E. S., and Mesirov, J. P. (2005). Gene set enrichment analysis: a knowledge-based approach for interpreting genome-wide expression profiles. Proc Natl Acad Sci U S A *102*, 15545-15550.

Tassone, P., Neri, P., Carrasco, D. R., Burger, R., Goldmacher, V. S., Fram, R., Munshi, V., Shammas, M. A., Catley, L., Jacob, G. S.*, et al.* (2005). A clinically relevant SCID-hu in vivo model of human multiple myeloma. Blood *106*, 713-716.

Van den Berg, C. L., McGill, J. R., Kuhn, J. G., Walsh, J. T., De La Cruz, P. S., Davidson, K. K., Wahl, G. M., and Von Hoff, D. D. (1994). Pharmacokinetics of hydroxyurea in nude mice. Anticancer Drugs *5*, 573-578.

Wang, Z., Raifu, M., Howard, M., Smith, L., Hansen, D., Goldsby, R., and Ratner, D. (2000). Universal PCR amplification of mouse immunoglobulin gene variable regions: the design of degenerate primers and an assessment of the effect of DNA polymerase 3' to 5' exonuclease activity. J Immunol Methods *233*, 167-177.

Figure S1. Transgenic MYC mRNA expression in transfected 293-T cells.
RT-PCR was performed on cDNA from 293T cells un-transfected, or transfected with CMV-MYC or CMV*MYC plasmids, using a forward primer downstream the CMV promoter and reverse primers in exon 3 of MYC, or, as a control, using actin specific primers. A no DNA control was also performed (- control).

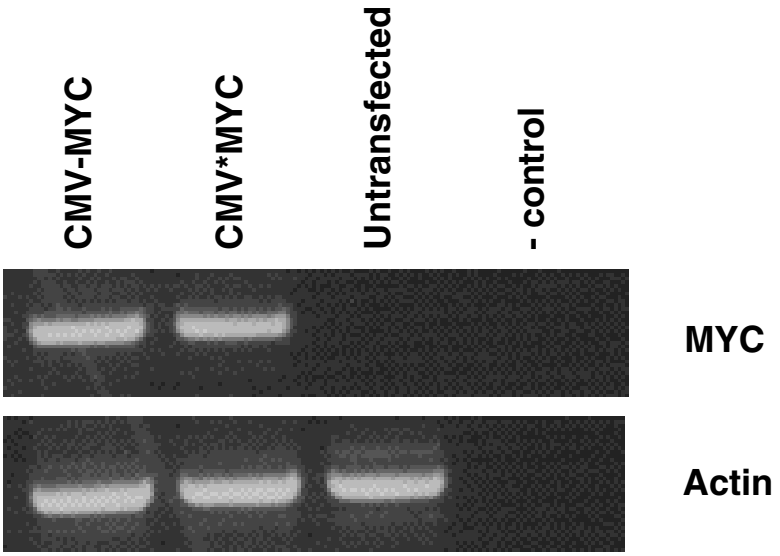

Figure S2. LPS treatment of Vk*MYC splenocytes induces PC differentiation. FCM analysis, performed on Vk*MYC splenocytes left untreated at day 0 (-) or treated for five days in LPS (+), identify increased PC population ($CD138^{+}$) upon LPS stimulation.

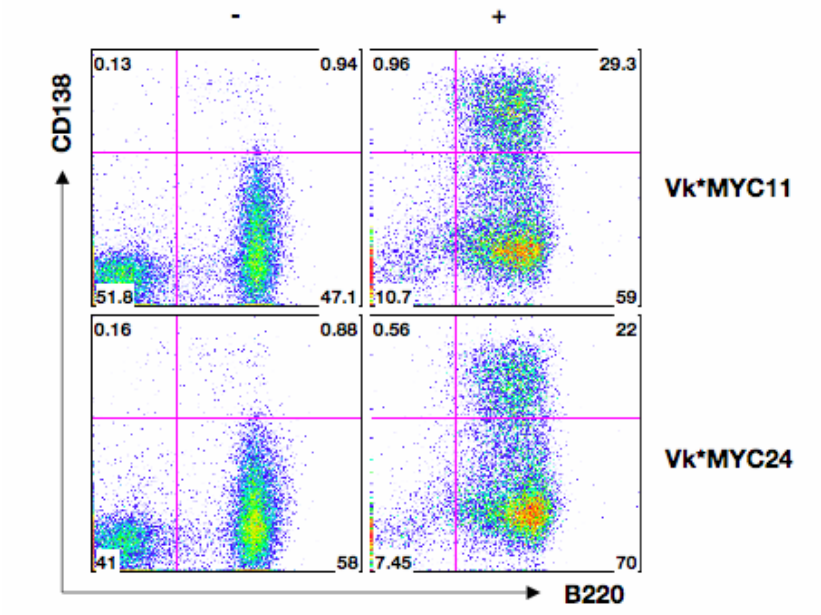

Figure S3. Isotype specific Ig ELISA performed on 70 weeks old sera from a cohort of 82 WT and Vk*MYC mice. ELISA determinations of serum Ig subtypes are shown on a logarithmic plot, bars represent median levels. Medians with 95% confidence intervals are shown below along with their p values if significant. IgG2c is the IgG2a equivalent in C57BL/6 mice.

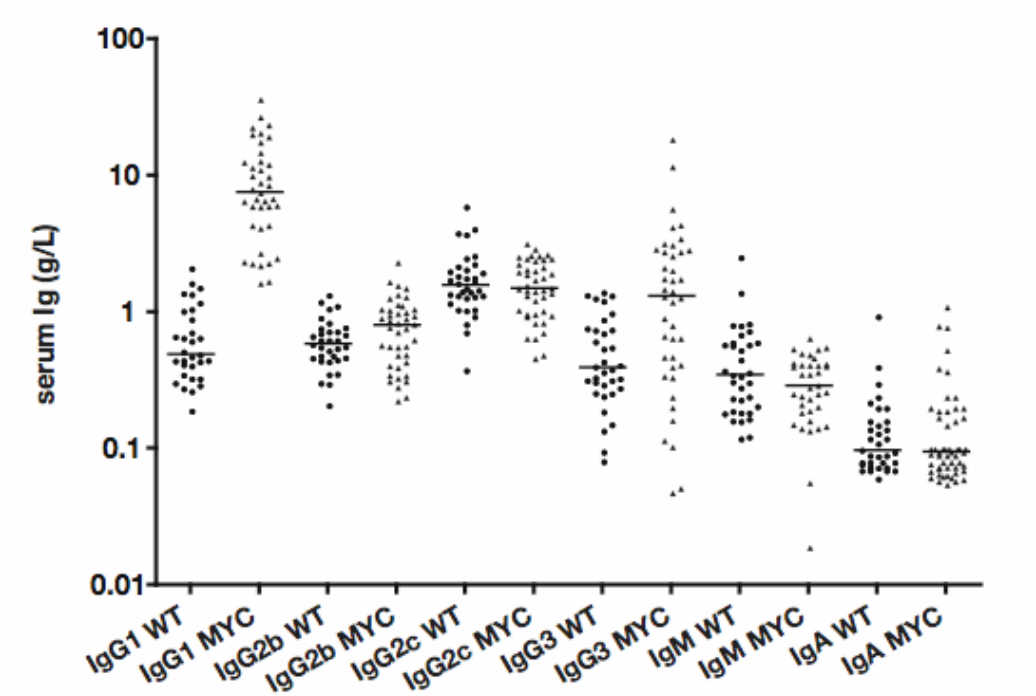

	Wild Type	MYC	p value
IgG1	0.491 (0.352-1.027)	9.107 (4.37-14.09)	0.0032
IgG2b	0.589 (0.458-0.749)	0.802 (0.422-1.061)	0.04
IgG2c	1.583 (1.231-2.132)	1.430 (0.840-2.114)	ns
IgG3	0.394 (0.269-0.759)	1.320 (0.408-2.844)	0.0049
IgM	0.347 (0.188-0.605)	0.254 (0.142-0.422)	ns
IgA	0.097 (0.076-0.940)	0.095 (0.073-1.100)	ns

Figure S4. Plasmacytoma in Vk*MYC mice.

H&E staining of a spleen section from an aged Vk*MYC mouse with PCT is shown. From the same mouse, $B220^{+}/CD138^{+}$ tumor cells are detected by flow cytometry in spleen, LN and BM.

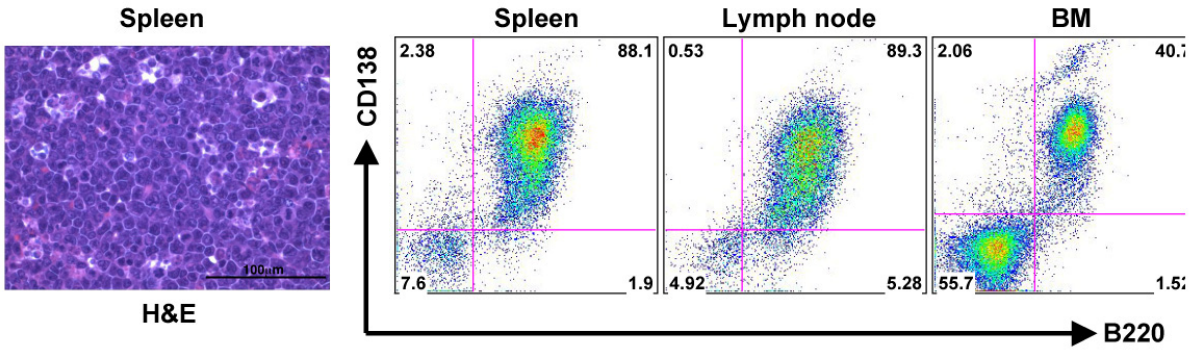

Figure S5. Burkitt's lymphoma in Vk*MYC mice.
A) Lymphoma cells in spleen sections from an aged Vk*MYC mouse were double stained with MYC (nuclear blue staining) and B220 (brown membrane). On the same tissue, flow cytometric analysis identifies class switched tumor B cells

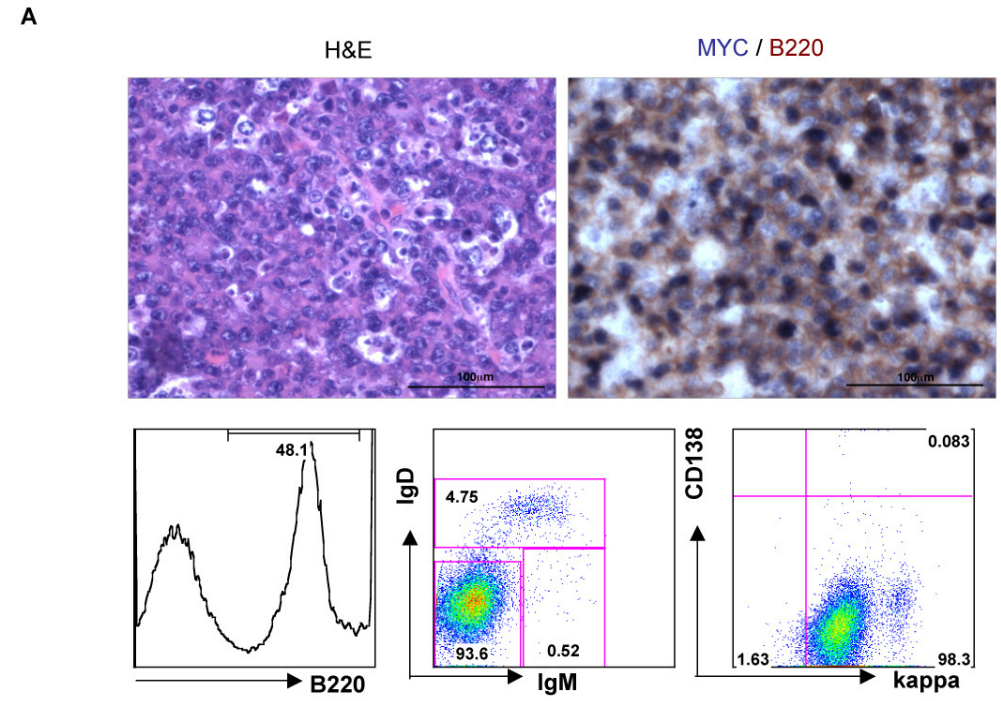

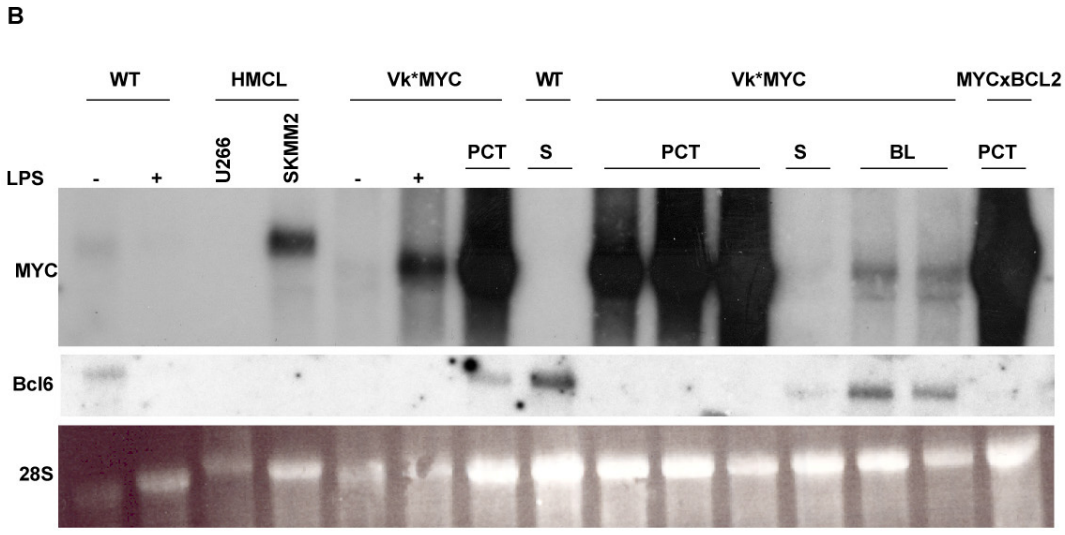

Figure S6. The University of Arkansas Dataset is arrange according to stage of PC neoplasm and ascending order of the MYC index. MYC index is not present in normal PCs, rarely present in MGUS, present in the majority of MM and almost all of the cell lines. There is good correlation with *MYC* expression and proliferation. The color scale for the heat-map is similar to that use in figure 6B.

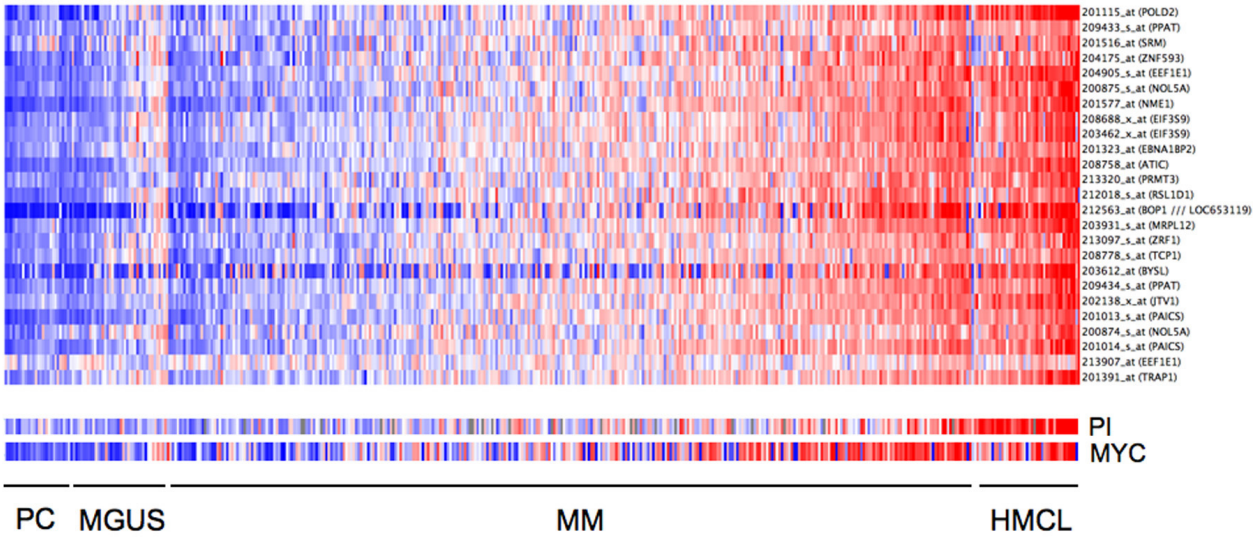

Table S1. Complete list of genesets used for GSEA and their enrichment scores and significance values (*p* and *q* values).

NAME	SIZE	ES	NES	NOM p-val	FDR q-val
ZHAN_MM_CD138_PR_VS_REST	42	0.82	3.10	0	0
CANCER_UNDIFFERENTIATED_META_UP	67	0.72	3.02	0	0
SERUM_FIBROBLAST_CELLCYCLE	110	0.63	2.89	0	0
TARTE_PLASMA_BLASTIC	305	0.55	2.84	0	0
PENG_RAPAMYCIN_DN	188	0.57	2.83	0	0
MOOTHA_VOXPHOS	77	0.65	2.81	0	0
IDX_TSA_UP_CLUSTER3	83	0.64	2.80	0	0
LEE_TCELLS3_UP	93	0.63	2.76	0	0
P21_P53_ANY_DN	47	0.70	2.73	0	0
PENG_GLUTAMINE_DN	248	0.53	2.73	0	0
LI_FETAL_VS_WT_KIDNEY_DN	159	0.55	2.69	0	0
ELECTRON_TRANSPORT_CHAIN	90	0.61	2.67	0	0
MOREAUX_TACI_HI_IN_PPC_UP	56	0.66	2.67	0	0
HUMAN_MITODB_6_2002	379	0.50	2.66	0	0
DOX_RESIST_GASTRIC_UP	43	0.69	2.66	0	0
SCHUMACHER_MYC_UP	50	0.66	2.65	0	0
MOREAUX_TACI_HI_VS_LOW_DN	143	0.55	2.64	0	0
CMV_IE86_UP	49	0.67	2.61	0	0
MITOCHONDRIA	387	0.48	2.60	0	0
CROONQUIST_IL6_STARVE_UP	33	0.72	2.59	0	0
CANTHARIDIN_DN	49	0.66	2.57	0	0
PENG_LEUCINE_DN	139	0.54	2.56	0	0
SHIPP_FL_VS_DLBCL_DN	34	0.70	2.55	0	0
ADIP_DIFF_CLUSTER5	35	0.71	2.55	0	0
CANCER_NEOPLASTIC_META_UP	60	0.62	2.53	0	0
MENSSEN_MYC_UP	31	0.71	2.49	0	0
PRMT5_KD_UP	166	0.51	2.49	0	0
BRCA_PROGNOSIS_NEG	94	0.56	2.48	0	0
OXIDATIVE_PHOSPHORYLATION	55	0.61	2.46	0	0
SERUM_FIBROBLAST_CORE_UP	174	0.50	2.46	0	0
CROONQUIST_IL6_RAS_DN	24	0.74	2.45	0	0
LE_MYELIN_UP	82	0.56	2.45	0	0
HDACI_COLON_CUR48HRS_UP	60	0.59	2.44	0	0
CHANG_SERUM_RESPONSE_UP	143	0.52	2.44	0	0
INOS_ALL_UP	52	0.61	2.43	0	0
YU_CMYC_UP	27	0.71	2.40	0	0
IDX_TSA_UP_CLUSTER5	88	0.54	2.39	0	0
HESS_HOXAANMEIS1_UP	55	0.60	2.39	0	0
TARTE_PC	80	0.55	2.38	0	0
HESS_HOXAANMEIS1_DN	55	0.60	2.37	0	0
MANALO_HYPOXIA_DN	78	0.55	2.37	0	2.33E-05
REN_E2F1_TARGETS	36	0.65	2.36	0	2.27E-05
GOLDRATH_HP	129	0.50	2.35	0	2.22E-05
PROTEASOMEPATHWAY	21	0.74	2.35	0	2.17E-05
UVB_NHEK3_C7	53	0.59	2.32	0	2.12E-05
PGC	343	0.43	2.32	0	2.08E-05
VANTVEER_BREAST_OUTCOME_GOOD_VS_POOR_DN	63	0.55	2.32	0	2.03E-05
HOFFMANN_BIVSBII_BI_TABLE2	184	0.47	2.30	0	1.99E-05
P21_P53_MIDDLE_DN	23	0.69	2.30	0	1.95E-05
ZELLER_MYC_UP	23	0.70	2.29	0	1.91E-05
P21_MIDDLE_DN	15	0.77	2.27	0	1.87E-05
BREAST_DUCTAL_CARCINOMA_GENES	18	0.74	2.27	0	1.84E-05
BASSO_REGULATORY_HUBS	138	0.47	2.24	0	7.27E-05
BRCA1_OVEREXP_DN	109	0.49	2.24	0	8.94E-05
HDACI_COLON_BUT48HRS_DN	99	0.49	2.23	0	8.78E-05
MYC_TARGETS	39	0.60	2.21	0	1.03E-04
GREENBAUM_E2A_UP	32	0.62	2.21	0	1.02E-04

PROTEASOME	17	0.73	2.21	0	9.99E-05
BREASTCA_THREE_CLASSES	41	0.59	2.18	0	2.14E-04
AGUIRRE_PANCREAS_CHR7	48	0.55	2.17	0	2.27E-04
AGED_MOUSE_HYPOTH_UP	43	0.56	2.16	0	3.03E-04
UVB_NHEK2_UP	68	0.51	2.16	0	3.14E-04
SASAKI_TCELL_LYMPHOMA_VS_CD4_UP	167	0.44	2.15	0	3.25E-04
SASAKI_ATL_UP	167	0.44	2.15	0	3.35E-04
BREASTCA_TWO_CLASSES	131	0.45	2.15	0	3.45E-04
CELL_CYCLE	74	0.50	2.14	0	3.40E-04
HDACI_COLON_CUR_UP	99	0.47	2.14	0	3.79E-04
HCC_SURVIVAL_GOOD_VS_POOR_DN	121	0.46	2.13	0	4.73E-04
IDX_TSA_UP_CLUSTER6	146	0.45	2.12	0	4.66E-04
UVB_SCC_UP	86	0.49	2.12	0	4.60E-04
MRNA_SPLICING	47	0.54	2.12	0	4.53E-04
PENTOSE_PHOSPHATE_PATHWAY	23	0.64	2.10	0	6.22E-04
TRANSLATION_FACTORS	45	0.55	2.10	0	6.14E-04
HDACI_COLON_SUL24HRS_UP	55	0.53	2.09	0	6.84E-04
FERRANDO_MLL_T_ALL_DN	83	0.48	2.09	0	6.75E-04
ROME_INSULIN_2F_UP	167	0.43	2.08	0	7.29E-04
ZHAN_MULTIPLE_MYELOMA_SUBCLASSES_DIFF	30	0.60	2.08	0	7.19E-04
OLDAGE_DN	47	0.54	2.08	0	7.10E-04
UVB_NHEK3_C0	82	0.48	2.08	0	7.01E-04
ALCALAY_AML_NPMC_DN	187	0.42	2.07	0	8.62E-04
P21_ANY_DN	32	0.58	2.05	0	0.001029159
VERNELL_PRB_CLSTR1	53	0.51	2.05	0	0.001027884
ADIP_DIFF_CLUSTER4	32	0.58	2.04	0	0.001085465
ZHAN_MM_CD138_MF_VS_REST	42	0.53	2.04	0	0.001084641
HDACI_COLON_CUR24HRS_UP	36	0.55	2.03	0	0.001127643
BRENTANI_CELL_CYCLE	80	0.47	2.03	0	0.001193328
GOLDRATH_CELLCYCLE	27	0.60	2.03	0	0.001201563
KREBS_TCA_CYCLE	29	0.58	2.00	0	0.001670277
SANA_IFNG_ENDOTHELIAL_DN	80	0.47	2.00	0	0.001684279
N_GLYCAN_BIOSYNTHESIS	22	0.62	2.00	0	0.001697677
BLEO_MOUSE_LYMPH_HIGH_24HRS_DN	34	0.55	2.00	0	0.001741794
CELL_CYCLE_KEGG	80	0.46	1.99	0	0.001858858
BHATTACHARYA_ESC_UP	57	0.49	1.98	0	0.00215009
ET743_SARCOMA_48HRS_DN	169	0.40	1.97	0	0.002351496
CHAUHAN_2ME2	46	0.51	1.96	0	0.002528939
RCC_NL_UP	443	0.36	1.95	0	0.002832497
ELONGINA_KO_DN	154	0.41	1.95	0	0.002812752
GAY_YY1_DN	220	0.39	1.94	0	0.003274018
DNA_REPLICATION_REACTOME	44	0.51	1.94	0	0.003290746
ABRAHAM_AL_VS_MM_DN	18	0.63	1.93	0.003717472	0.003538064
MMS_MOUSE_LYMPH_HIGH_4HRS_UP	33	0.53	1.92	0.00189394	0.003952824
GOLUB_ALL_VS_AML_UP	19	0.61	1.92	0	0.004018251
VHL_NORMAL_UP	380	0.36	1.91	0	0.004167155
COLLER_MYC_UP	17	0.62	1.90	0.003724395	0.00502881
ET743_SARCOMA_72HRS_DN	202	0.38	1.90	0	0.004980917
PURINE_METABOLISM	111	0.42	1.90	0	0.005006948
PYRIMIDINE_METABOLISM	55	0.48	1.90	0	0.004987189
SHEPARD_GENES_COMMON_BW_CB_MO	60	0.46	1.89	0	0.005002198
MRNA_PROCESSING_REACTOME	102	0.42	1.89	0.001686341	0.005389058
GENOTOXINS_ALL_24HRS_REG	28	0.55	1.88	0	0.005723327
ZHAN_MMPC_SIM	42	0.49	1.88	0	0.005733455
GENOTOXINS_ALL_4HRS_REG	22	0.59	1.88	0.002028398	0.00579429
ABRAHAM_MM_VS_AL_UP	19	0.60	1.88	0.001838235	0.00581239
CITRATE_CYCLE_TCA_CYCLE	20	0.60	1.88	0	0.005778273
HSC_INTERMEDIATEPROGENITORS_SHARED	105	0.41	1.88	0	0.00580354
PYRUVATE_METABOLISM	35	0.52	1.86	0	0.006912691
UVB_NHEK3_ALL	390	0.34	1.85	0	0.008048993
TCA	15	0.64	1.84	0.007246377	0.008203072
IRITANI_ADPROX_UP	26	0.54	1.84	0.003710575	0.008175003
HDACI_COLON_BUT12HRS_DN	66	0.44	1.84	0	0.008147028
CMV_24HRS_UP	69	0.44	1.83	0	0.008914954

GENOTOXINS_4HRS_DISCR	33	0.51	1.83	0.001821494	0.008873353
HSC_INTERMEDIATEPROGENITORS_FETAL	124	0.39	1.83	0	0.008855553
IDX_TSA_UP_CLUSTER4	36	0.50	1.83	0	0.008861938
HSC_LATEPROGENITORS_SHARED	366	0.34	1.83	0	0.008806666
CMV_ALL_UP	90	0.42	1.83	0	0.009211202
HIPPOCAMPUS_DEVELOPMENT_PRENATAL	32	0.52	1.82	0.003710575	0.00943561
HSC_LATEPROGENITORS_ADULT	373	0.34	1.82	0	0.009491793
HDACI_COLON_BUT_DN	214	0.36	1.82	0	0.009582843
ZHAN_MM_CD138_CD1_VS_REST	33	0.51	1.82	0.003663004	0.009553432
JAIN_NEMO_DIFF	74	0.42	1.82	0	0.009553107
CARBON_FIXATION	20	0.56	1.81	0.003584229	0.010428136
IGFR_IR_UP	16	0.61	1.80	0.005199307	0.011201721
GLYCOLYSIS_AND_GLUCONEOGENESIS	42	0.48	1.80	0.001865672	0.011118126
ZHAN_MM_MOLECULAR_CLASSI_UP	47	0.46	1.80	0	0.011422573
HSC_LATEPROGENITORS_FETAL	373	0.34	1.79	0	0.01190787
VHL_RCC_UP	96	0.40	1.79	0	0.012088584
BUT_TSA_UP	18	0.59	1.79	0.009765625	0.012042929
ROTH_HTERT_DIFF	31	0.51	1.79	0.003490401	0.012429717
HDACI_COLON_SUL_UP	113	0.39	1.79	0	0.012375249
VENTRICLES_UP	205	0.36	1.78	0	0.012418152
ET743_SARCOMA_DN	246	0.35	1.78	0	0.013107829
PEART_HISTONE_DN	71	0.42	1.78	0.001697793	0.013159758
RNA_TRANSCRIPTION_REACTOME	34	0.48	1.77	0.005405406	0.013374713
H2O2_CSBDIFF_C2	33	0.50	1.77	0.007434944	0.013328473
HEARTFAILURE_ATRIA_DN	110	0.39	1.77	0.001745201	0.013866496
IFN_BETA_GLIOMA_DN	44	0.46	1.76	0.001808318	0.015754446
ZHAN_MULTIPLE_MYELOMA_VS_NORMAL_UP	62	0.43	1.75	0.003571429	0.015831124
MITOCHONDRIAL_FATTY_ACID_BETAOXIDATION	16	0.57	1.75	0.003968254	0.015835222
HSC_INTERMEDIATEPROGENITORS_ADULT	114	0.38	1.75	0	0.015962144
ALZHEIMERS_INCIPIENT_DN	144	0.36	1.75	0	0.016029198
HYPOXIA_RCC_NOVHL_UP	57	0.44	1.74	0	0.01730221
AGUIRRE_PANCREAS_CHR8	61	0.42	1.74	0	0.01760951
NING_COPD_DN	111	0.38	1.74	0.001650165	0.017927483
WANG_MLL_CBP_VS_GMP_DN	38	0.46	1.74	0.007246377	0.018067269
BAF57_BT549_DN	313	0.33	1.74	0	0.018037444
XU_CBP_UP	19	0.55	1.73	0.014112903	0.01802659
HSC_EARLYPROGENITORS_ADULT	344	0.33	1.73	0	0.018119622
HSC_EARLYPROGENITORS_SHARED	342	0.33	1.73	0	0.018297113
HSC_EARLYPROGENITORS_FETAL	342	0.33	1.73	0	0.0186354
GLYCOLYSIS	49	0.44	1.73	0	0.01883528
SMITH_HTERT_UP	102	0.38	1.72	0.001745201	0.019667976
CELL_CYCLE_CHECKPOINT	24	0.51	1.72	0.014336918	0.019772658
STEMCELL_COMMON_UP	153	0.36	1.72	0	0.020046761
HUMAN_TISSUE_TESTIS	59	0.42	1.72	0.001683502	0.020141903
HDACI_COLON_SUL12HRS_UP	20	0.53	1.71	0.016304348	0.02055139
GLUCONEOGENESIS	49	0.44	1.71	0.003571429	0.020742323
PROTEASOME_DEGRADATION	31	0.48	1.71	0.007366483	0.021307316
PENG_GLUCOSE_DN	133	0.36	1.70	0	0.021958588
CORTEX_ENRICHMENT_LATE_UP	19	0.54	1.70	0.015209125	0.02184057
CAMPTOTHECIN_PROBCELL_DN	28	0.49	1.70	0.013207547	0.022760838
HDACI_COLON_BUT16HRS_DN	97	0.38	1.70	0.001669449	0.022774203
HDACI_COLON_SUL48HRS_UP	79	0.40	1.70	0	0.023239756
HASLINGER_B_CLL_17P13	16	0.57	1.69	0.013513514	0.024757523
HBX_HEP_UP	18	0.55	1.69	0.013358778	0.02499172
TNFALPHA_4HRS_UP	39	0.45	1.69	0.006944445	0.024855413
HDACI_COLON_CLUSTER5	21	0.52	1.68	0.015037594	0.024926933
PHOTOSYNTHESIS	20	0.53	1.68	0.015594542	0.024905723
ET743_SARCOMA_72HRS_UP	62	0.41	1.68	0.007017544	0.025031088
FLAGELLAR_ASSEMBLY	19	0.54	1.68	0.016697587	0.025283005
HDACI_COLON_CURSUL_UP	37	0.46	1.68	0.001841621	0.025531368
CIS_XPC_UP	143	0.35	1.68	0.001697793	0.025783401
TYPE_III_SECRETION_SYSTEM	19	0.54	1.67	0.009363296	0.02760692
BRCA1_SW480_UP	25	0.50	1.66	0.023809524	0.029596748
OLDONLY_FIBRO_UP	34	0.46	1.66	0.005484461	0.02987458

ATP_SYNTHESIS	19	0.54	1.65	0.016574586	0.030638322
GH_HYPOPHYSECTOMY_RAT_DN	15	0.57	1.65	0.009560229	0.031625155
RIBOSOMAL_PROTEINS	92	0.37	1.65	0	0.03169459
SHEPARD_CRASH_AND_BURN_MUT_VS_WT_DN	137	0.35	1.64	0.001730104	0.033303637
KLEIN_PEL_UP	50	0.42	1.64	0.010676157	0.03376282
AGUIRRE_PANCREAS_CHR12	59	0.40	1.64	0.007407407	0.0349929
MRNA_PROCESSING	41	0.43	1.64	0.007220217	0.03526695
ZHAN_MMPC_SIMAL	47	0.43	1.63	0.007207207	0.035529274
GH_GHRHR_KO_24HRS_DN	141	0.34	1.63	0	0.035356108
FATTY_ACID_DEGRADATION	24	0.49	1.63	0.013059702	0.035777893
HBX_HCC_UP	16	0.55	1.63	0.011516315	0.03562961
BRCA_BRCA1_POS	95	0.36	1.60	0.005405406	0.0462715
FERNANDEZ_MYC_TARGETS	178	0.33	1.59	0.0016	0.05008947
YAGI_AML_PROGNOSIS	34	0.43	1.59	0.011516315	0.050971057
ET743_SARCOMA_24HRS_DN	95	0.35	1.58	0.006802721	0.052692626
ATRBRCAPATHWAY	20	0.50	1.58	0.02264151	0.05261808
FLECHNER_KIDNEY_TRANSPLANT_WELL_PBL_UP	152	0.33	1.58	0.001666667	0.052752823
BRCA1_OVEREXP_UP	157	0.32	1.58	0	0.052911513
AGEING_KIDNEY_SPECIFIC_DN	120	0.34	1.58	0.001642036	0.052892376
LEI_MYB_REGULATED_GENES	317	0.30	1.58	0	0.0534491
BYSTRYKH_HSC_BRAIN_CIS_GLOCUS	41	0.41	1.57	0.015151516	0.054143
BLEO_MOUSE_LYMPH_LOW_24HRS_DN	24	0.47	1.57	0.03649635	0.055562105
TPA_SKIN_UP	16	0.53	1.57	0.035185184	0.05581307
SHEPARD_BMYB_MORPHOLINO_DN	152	0.33	1.57	0.003338898	0.057202503
LIN_WNT_UP	53	0.39	1.56	0.017094018	0.057705253
CROONQUIST_IL6_RAS_UP	21	0.49	1.56	0.028680688	0.059155278
HYPOPHYSECTOMY_RAT_DN	48	0.40	1.55	0.016157988	0.06363306
ROS_MOUSE_AORTA_UP	22	0.47	1.55	0.036121674	0.06499694
NOUZOVA_CPG_H4_UP	95	0.35	1.54	0.009983361	0.06516317
HDACI_COLON_CUR12HRS_UP	16	0.52	1.54	0.04347826	0.06895444
HDACI_COLON_SUL30MIN_DN	32	0.44	1.54	0.040665433	0.068803616
POD1_KO_UP	339	0.29	1.53	0	0.069974914
UVB_NHEK1_C1	51	0.39	1.53	0.016917294	0.07056601
ALANINE_AND_ASPARTATE_METABOLISM	19	0.50	1.53	0.05464481	0.07030103
UBIQUITIN_MEDIATED_PROTEOLYSIS	22	0.48	1.53	0.040152963	0.07112323
UVB_NHEK1_UP	173	0.31	1.53	0.004854369	0.07208803
G1_TO_S_CELL_CYCLE_REACTOME	64	0.36	1.52	0.012216405	0.073531404
CHOLESTEROL_BIOSYNTHESIS	15	0.54	1.52	0.04779412	0.07412759
HYPOXIA_RCC_UP	86	0.35	1.52	0.011764706	0.07777655
HIPPOCAMPUS_DEVELOPMENT_POSTNATAL	44	0.40	1.52	0.018900344	0.07743534
MMS_HUMAN_LYMPH_LOW_4HRS_DN	16	0.50	1.51	0.0498155	0.08027374
MUNSHI_MM_VS_PCS_UP	76	0.36	1.51	0.010989011	0.08205971
OXSTRESS_RPE_H2O2HNE_DN	31	0.43	1.50	0.02329749	0.08388472
NEMETH_TNF_DN	29	0.43	1.50	0.030710172	0.0844005
PROPANOATE_METABOLISM	30	0.43	1.50	0.035778176	0.08448387
BRENTANI_REPAIR	35	0.41	1.50	0.029038113	0.08456307
PENG_GLUTAMINE_UP	227	0.29	1.50	0.001642036	0.08605867
CHEN_HOXA5_TARGETS_DN	47	0.38	1.50	0.02559415	0.086099
SANSOM_APC_LOSS5_UP	70	0.35	1.49	0.026223777	0.08874806
ADIP_VS_FIBRO_DN	27	0.43	1.49	0.030852994	0.08901177
TNFALPHA_ALL_UP	74	0.35	1.49	0.020689655	0.08924277
STANELLE_E2F1_UP	28	0.43	1.49	0.03409091	0.089364335
OLD_FIBRO_UP	55	0.37	1.48	0.04107143	0.0920248
ET743_SARCOMA_UP	65	0.36	1.48	0.02173913	0.095187
CPR_NULL_LIVER_UP	32	0.40	1.47	0.047186933	0.0973404
GENOTOXINS_24HRS_DISCR	35	0.40	1.46	0.040139616	0.11062187
IRS1_KO_ADIP_UP	84	0.33	1.45	0.027777778	0.11332708
WALLACE_JAK2_DIFF	30	0.41	1.45	0.054744527	0.11554826
IRITANI_ADPROX_LYMPH	125	0.31	1.45	0.01010101	0.11685039
ROSS_AML1_ETO	82	0.33	1.45	0.028070176	0.11695751
UVB_NHEK3_C6	29	0.42	1.44	0.040665433	0.118048966
BCNU_GLIOMA_NOMGMT_48HRS_DN	31	0.41	1.44	0.06440072	0.1201696
TIS7_OVEREXP_DN	17	0.48	1.44	0.06870229	0.120964766
HDACI_COLON_BUT30MIN_DN	32	0.40	1.44	0.06428572	0.12068423

MUNSHI_MM_UP	65	0.35	1.44	0.025641026	0.121558465
ZHAN_MM_CD138_HP_VS_REST	40	0.37	1.43	0.056437388	0.12378474
BRCA2_BRCA1_UP	47	0.37	1.43	0.067669176	0.12335087
HDACI_COLON_SUL16HRS_UP	37	0.38	1.43	0.0375	0.12525345
REOVIRUS_HEK293_UP	235	0.28	1.42	0.007874016	0.12979598
HDACI_COLON_BUT24HRS_DN	95	0.32	1.42	0.038333334	0.12958416
BRCA1_OVEREXP_PROSTATE_UP	154	0.30	1.42	0.008635579	0.12917262
IFNA_UV-CMV_COMMON_HCMV_6HRS_UP	29	0.41	1.42	0.063716814	0.13031676
UVC_HIGH_D3_DN	46	0.36	1.42	0.047368422	0.13152233
AGED_RHESUS_DN	107	0.31	1.42	0.03372681	0.13415444
ADIP_VS_FIBRO_UP	34	0.39	1.41	0.062166963	0.13655314
BYSTRYKH_HSC_BRAIN_TRANS_GLOCUS	143	0.30	1.41	0.018867925	0.14368303
PEART_HISTONE_UP	51	0.35	1.40	0.056985293	0.14472216
SANSOM_APC_LOSS4_UP	100	0.31	1.40	0.03380783	0.14720246
ADIP_DIFF_CLUSTER3	32	0.39	1.40	0.0704501	0.15160862
LEE_TCELLS10_UP	136	0.29	1.39	0.019323671	0.15196663
DER_IFNG_UP	61	0.33	1.39	0.03539823	0.15423451
PITUITARY_FETAL_UP	15	0.48	1.39	0.107344635	0.1557573
IFN_BETA_UP	65	0.33	1.39	0.054421768	0.15864058
LIZUKA_G1_SM_G2	25	0.42	1.39	0.08273381	0.15852828
BRCA1_OVEREXP_PROSTATE_DN	77	0.32	1.38	0.053819444	0.16193706
STRESS_ARSENIC_SPECIFIC_UP	144	0.29	1.38	0.025	0.16394393
JISON_SICKLECELL_DIFF	367	0.26	1.38	0.004716981	0.16395292
LEE_TCELLS8_UP	136	0.29	1.38	0.019900497	0.16423085
NAB_LUNG_UP	26	0.42	1.38	0.09057971	0.16448195
RUIZ_TENASCIN_TARGETS	79	0.32	1.36	0.04418985	0.17596233
MTORPATHWAY	23	0.41	1.36	0.10150376	0.17702372
HEARTFAILURE_VENTRICLE_DN	66	0.33	1.36	0.04244482	0.17676452
DER_IFNB_UP	91	0.31	1.36	0.028368793	0.17977466
LEE_TCELLS1_UP	136	0.29	1.36	0.038961038	0.18087195
LIZUKA_L0_SM_L1	19	0.44	1.36	0.1163227	0.18137611
CHEMICALPATHWAY	21	0.43	1.36	0.12099644	0.18248937
ZHAN_MMPC_SIM_BC_AND_MM	44	0.36	1.35	0.088652484	0.18551688
ADIP_VS_PREADIP_DN	37	0.37	1.35	0.10037879	0.18593219
UVB_NHEK2_DN	81	0.31	1.35	0.055652175	0.18554826
IFNALPHA_HCC_UP	29	0.38	1.35	0.1007326	0.18742204
IFNA_HCMV_6HRS_UP	53	0.34	1.35	0.0685413	0.19068182
UEDA_MOUSE_LIVER	119	0.29	1.35	0.034602076	0.19055003
CMV_HCMV_TIMECOURSE_14HRS_UP	44	0.35	1.34	0.08256881	0.19876373
ERM_KO_TESTES_DN	17	0.44	1.33	0.116981134	0.20221426
ZUCCHI_EPITHELIAL_UP	41	0.35	1.33	0.10382514	0.20718417
IFNALPHA_RESIST_DN	18	0.44	1.33	0.10507246	0.2098148
LYSINE_DEGRADATION	28	0.39	1.33	0.115173675	0.21032517
AGED_MOUSE_CORTEX_DN	44	0.34	1.32	0.088607594	0.21793371
TPA_RESIST_EARLY_DN	74	0.31	1.32	0.07599309	0.21823022
IFN_ANY_UP	81	0.30	1.32	0.062068965	0.2181319
KIM_TH_CELLS_UP	44	0.34	1.31	0.10106383	0.22216928
CELLCYCLEPATHWAY	22	0.41	1.31	0.13628319	0.22326706
STRESS_ARSENIC_SPECIFIC_DN	27	0.39	1.31	0.14174758	0.22727606
AS3_FIBRO_C3	43	0.34	1.31	0.1090573	0.22881982
AGEING_KIDNEY_DN	110	0.29	1.31	0.05882353	0.22910593
REOVIRUS_HEK293_DN	230	0.26	1.31	0.032407407	0.22901449
HDACI_COLON_TSA_DN	55	0.33	1.30	0.09547739	0.23358172
AS3_FIBRO_UP	43	0.34	1.30	0.09380863	0.23458819
ET743_RESIST_UP	17	0.43	1.30	0.14705883	0.24111728
CALRES_MOUSE_DN	39	0.35	1.29	0.10928962	0.2433936
HG_PROGERIA_DN	25	0.38	1.29	0.121442124	0.25086945
HDACI_COLON_SUL16HRS_DN	64	0.31	1.29	0.11940298	0.251782
SMITH_HCV_INDUCED_HCC_UP	33	0.36	1.28	0.13114753	0.25767258
ELECTRON_TRANSPORTER_ACTIVITY	106	0.29	1.28	0.067226894	0.25731993
HBX_NL_UP	22	0.39	1.28	0.15213358	0.2576881
TNFALPHA_ADIP_DN	54	0.32	1.28	0.119929455	0.26219052
VEGFPATHWAY	27	0.37	1.28	0.14338236	0.26336208
TSA_CD4_UP	25	0.38	1.27	0.14684016	0.26607698

AMINOACYL_TRNA_BIOSYNTHESIS	21	0.39	1.27	0.16489361	0.2659821
DEATHPATHWAY	32	0.36	1.27	0.15116279	0.26788685
HDACI_COLON_TSABUT_DN	19	0.41	1.27	0.15970962	0.27143428
UVB_NHEK3_C1	56	0.31	1.27	0.13438046	0.27604073
POMEROY_DESMOPLASIC_VS_CLASSIC_MD_DN	41	0.33	1.26	0.13435374	0.2771665
AGED_MOUSE_NEOCORTEX_UP	61	0.31	1.26	0.105902776	0.2766321
EGF_HDMEC_UP	42	0.33	1.26	0.13676731	0.2770101
ADIPOCYTE_PPARG_UP	15	0.44	1.26	0.18450184	0.27972072
ET743_SARCOMA_6HRS_UP	30	0.36	1.26	0.14183123	0.2833165
AGUIRRE_PANCREAS_CHR17	70	0.30	1.25	0.12280702	0.29218352
HOFFMANN_BIVSBII_LGBII	90	0.29	1.25	0.09966216	0.29351613
CPR_LOW_LIVER_DN	21	0.39	1.25	0.17331022	0.2931725
IGF1MTORPATHWAY	20	0.39	1.25	0.17805755	0.29235947
WONG_IFNA_HCC_RESISTANT_VS_SENSITIVE_DN	30	0.36	1.25	0.17321429	0.29162458
MITOCHONDRIAPATHWAY	20	0.39	1.24	0.18691589	0.29998204
TRNA_SYNTHETASES	18	0.40	1.24	0.18726592	0.30272856
POMEROY_MD_TREATMENT_GOOD_VS_POOR_DN	24	0.38	1.24	0.16666667	0.30703554
RADAEVA_IFNA_UP	50	0.31	1.23	0.1590909	0.316194
GN_CAMP_GRANULOSA_UP	53	0.31	1.23	0.16157989	0.31859285
MATSUDA_VALPHAINKT_DIFF	361	0.23	1.23	0.040971167	0.31788507
TSA_HEPATOMA_UP	33	0.34	1.23	0.163606	0.32315037
BYSTRYKH_HSC_CIS_GLOCUS	91	0.28	1.23	0.11764706	0.32247385
APPEL_IMATINIB_UP	31	0.34	1.23	0.16955018	0.32362154
DAC_IFN_BLADDER_UP	16	0.41	1.23	0.21904762	0.3232535
CPR_LOW_LIVER_UP	16	0.42	1.22	0.21245421	0.3229284
APOPTOSIS	67	0.29	1.22	0.1498195	0.3222728
BRCA1_MES_UP	38	0.33	1.22	0.18249534	0.3228098
IFNALPHA_NL_UP	27	0.36	1.22	0.16666667	0.32702482
ET743_RESIST_DN	40	0.33	1.22	0.17081851	0.32800913
GOLUB_ALL_VS_AML_DN	16	0.41	1.22	0.20190476	0.3280731
DER_IFNA_UP	65	0.29	1.22	0.14159292	0.3324737
H2O2_CSBRESCUED_UP	54	0.30	1.21	0.15318416	0.33426303
CELL_CYCLE_REGULATOR	24	0.37	1.21	0.19921105	0.33658433
TNFALPHA_TGZ_ADIP_DN	25	0.36	1.21	0.1996337	0.33781764
IDX_TSA_UP_CLUSTER2	58	0.30	1.21	0.15547703	0.3436753
ET743_HELA_DN	15	0.42	1.21	0.22003578	0.34331873
VALINE_LEUCINE_AND_ISOLEUCINE_DEGRADATION	35	0.33	1.20	0.20220588	0.34921092
IGLESIAS_E2FMINUS_UP	136	0.26	1.20	0.13311689	0.34855923
TSADAC_HYPOMETH_OVCA_UP	39	0.32	1.20	0.19031142	0.35360616
BRACX_UP	19	0.39	1.20	0.22605364	0.3594046
CMV_HCMV_TIMECOURSE_12HRS_UP	26	0.36	1.20	0.20222634	0.35946044
HIPPOCAMPUS_DEVELOPMENT_NEONATAL	26	0.36	1.19	0.21582733	0.3599319
DIAB_NEPH_DN	373	0.22	1.19	0.07763975	0.36030033
YAGI_AML_PROG_FAB	190	0.24	1.19	0.14125201	0.35950917
SHIPP_DLBCL_CURED_DN	36	0.32	1.19	0.20255475	0.366761
RIBAVIRIN_RSV_UP	22	0.37	1.19	0.2238806	0.36662847
FLECHNER_KIDNEY_TRANSPLANT_WELL_DN	22	0.37	1.19	0.22557727	0.3702787
HSC_MATURE_FETAL	251	0.23	1.19	0.08557845	0.37223974
H2O2_CSBDIFF_C1	32	0.33	1.18	0.20257826	0.37405315
HSC_MATURE_SHARED	202	0.24	1.18	0.1221865	0.3776097
GH_EXOGENOUS_EARLY_UP	24	0.36	1.18	0.25985664	0.3871415
CMV_HCMV_TIMECOURSE_10HRS_DN	15	0.40	1.17	0.25795054	0.3919267
LEE_MYC_E2F1_UP	55	0.29	1.17	0.19791667	0.39156455
GLUTATHIONE_METABOLISM	28	0.34	1.17	0.24	0.3941512
MARSHALL_SPLEEN_BAL	20	0.37	1.17	0.23562153	0.39408806
P38MAPKPATHWAY	39	0.32	1.17	0.21869488	0.39491343
BENNETT_SLE_UP	28	0.34	1.17	0.23135756	0.39421102
HOFMANN_MDS_CD34_LOW_AND_HIGH_RISK	46	0.30	1.17	0.22014925	0.39360502
UVC_HIGH_D1_DN	15	0.40	1.17	0.27946767	0.39551514
CHESLER_BRAIN_CIS_GENES	50	0.29	1.17	0.214539	0.3946673
UVC_HIGH_D2_DN	37	0.32	1.17	0.21621622	0.39721996
HOUSTIS_ROS	30	0.33	1.16	0.26047358	0.39817935
H2O2_CSBRESCUED_C1_UP	40	0.31	1.16	0.21481481	0.3979789
NADLER_OBESITY_DN	33	0.32	1.16	0.2589928	0.40269905

G2PATHWAY	23	0.35	1.16	0.2580645	0.4034565
LIZUKA_G2_GR_G3	26	0.34	1.16	0.2580071	0.40963697
AGED_MOUSE_HYPOTH_DN	37	0.31	1.16	0.24729241	0.41105127
GAMMA-UV_FIBRO_UP	32	0.33	1.15	0.26055047	0.41147408
HSC_MATURE_ADULT	270	0.22	1.15	0.13535032	0.4119127
FALT_BCLL_DN	49	0.29	1.15	0.22767076	0.41371992
FATTY_ACID_METABOLISM	79	0.27	1.15	0.21808511	0.412678
UVC_XPCS_8HR_UP	58	0.28	1.15	0.23090586	0.4168564
PENG_RAPAMYCIN_UP	154	0.24	1.15	0.1724138	0.4178517
TPA_SENS_LATE_DN	232	0.22	1.14	0.15797788	0.42566833
BYSTROM_IL5_DN	56	0.29	1.14	0.23518851	0.42564398
NING_COPD_UP	142	0.24	1.14	0.19897959	0.4427573
CHAUVIN_ANDROGEN_REGULATED_GENES	43	0.30	1.13	0.26070765	0.44320032
LEE_MYC_UP	53	0.28	1.13	0.26032317	0.4424615
UV-4NQO_FIBRO_UP	28	0.33	1.13	0.2820513	0.4416947
NI2_LUNG_DN	19	0.36	1.13	0.28782287	0.4417987
HIF1_TARGETS	35	0.31	1.13	0.2895204	0.4498163
CHEN_LUNG_SURVIVAL	20	0.36	1.13	0.30111524	0.45098764
GH_GHRHR_KO_6HRS_DN	30	0.32	1.13	0.28028932	0.4502482
BUTANOATE_METABOLISM	27	0.33	1.13	0.3003663	0.45439932
SHEPARD_BMYB_MORPHOLINO_UP	137	0.24	1.12	0.21896552	0.4584346
UVB_NHEK3_C8	65	0.27	1.12	0.24390244	0.46261555
DSRNA_UP	37	0.31	1.12	0.2872928	0.46939778
DNA_DAMAGE_SIGNALING	87	0.25	1.12	0.26047358	0.46991003
LEE_E2F1_DN	62	0.27	1.12	0.252809	0.46939626
IFN_ALPHA_UP	40	0.30	1.12	0.29874778	0.46890107
GLUTAMATE_METABOLISM	23	0.34	1.11	0.29174665	0.4798727
BRENTANI_TRANSPORT_OF_VESICLES	23	0.34	1.11	0.30866808	0.480775
BRENTANI_DNA_METHYLATION_AND_MODIFICATION	23	0.34	1.10	0.34026465	0.4900169
LEE_TCELLS5_UP	17	0.36	1.10	0.32821497	0.49552163
CMV_UV-CMV_COMMON_HCMV_6HRS_UP	20	0.35	1.10	0.32958803	0.49647182
IFNALPHA_NL_HCC_UP	18	0.35	1.10	0.29444444	0.5025935
PENG_GLUCOSE_UP	33	0.30	1.10	0.3148148	0.5020928
HOGERKORP_CD44_DN	21	0.35	1.10	0.34837544	0.5033451
DORSAM_HOXA9_UP	31	0.31	1.10	0.3102837	0.5049256
MENSE_HYPOXIA_TRANSPORTER_GENES	37	0.30	1.09	0.3138686	0.5053324
BYSTROM_IL5_UP	39	0.29	1.09	0.29643527	0.50427616
HASLINGER_B_CLL_13Q14	19	0.36	1.09	0.33153152	0.5105894
FSH_OVARY_MCV152_DN	46	0.28	1.09	0.30871212	0.5123166
IFN_GAMMA_UP	38	0.30	1.09	0.32807016	0.5128402
BROCKE_IL6	144	0.23	1.09	0.2685624	0.5138257
HYPOXIA_NORMAL_UP	196	0.22	1.09	0.25080907	0.51363254
UVC_XPCS_ALL_UP	61	0.26	1.08	0.30208334	0.5199693
ESR_FIBROBLAST_UP	50	0.28	1.08	0.31323284	0.51919967
NI2_MOUSE_DN	41	0.28	1.08	0.31215972	0.52267265
KRETZSCHMAR_IL6_DIFF	144	0.23	1.08	0.28	0.5278731
CREB_BRAIN_2WKS_UP	21	0.34	1.08	0.37078652	0.5285295
CMV_HCMV_6HRS_UP	25	0.32	1.08	0.34234235	0.5294813
LEE_TCELLS9_UP	28	0.30	1.08	0.325	0.52838284
ZHAN_TONSIL_BONEMARROW	41	0.28	1.08	0.31491712	0.5296807
GH_AUTOCRINE_UP	180	0.22	1.07	0.2912458	0.53474844
RASPATHWAY	22	0.33	1.07	0.34854016	0.5396525
CHESLER_HIGHEST_FOLD_RANGE_GENES	33	0.29	1.07	0.35945484	0.54170585
EIF4PATHWAY	24	0.31	1.07	0.35809523	0.5444444
HTERT_UP	58	0.26	1.06	0.36476868	0.55260706
GALE_FLT3ANDAPL_UP	59	0.26	1.06	0.33453238	0.55450064
OKUMURA_MC_LPS	185	0.21	1.06	0.33277312	0.56161565
SHEPARD_CRASH_AND_BURN_MUT_VS_WT_UP	137	0.22	1.06	0.3204047	0.56051594
OXSTRESS_RPETWO_DN	108	0.23	1.06	0.33561644	0.56095964
LEI_HOXC8_DN	15	0.36	1.06	0.40409684	0.56334925
UVC_HIGH_D9_DN	24	0.31	1.05	0.36479127	0.5678764
IFN_ALL_UP	18	0.34	1.05	0.36720142	0.5674758
ZHAN_MMPC_LATEVS	45	0.27	1.05	0.36612022	0.5662581
HDACI_COLON_CLUSTER6	33	0.30	1.05	0.38309354	0.573715

JISON_SICKLE_CELL	31	0.30	1.05	0.35957065	0.5744564
CMV_8HRS_UP	31	0.30	1.05	0.3874046	0.57529014
GH_AUTOCRINE_DN	107	0.23	1.05	0.3303887	0.57847595
OLDWERNER_FIBRO_DN	101	0.23	1.05	0.35506004	0.5814983
CROMER_HYPOPHARYNGEAL_MET_VS_NON_UP	71	0.24	1.04	0.3631579	0.58344007
CROMER_HYPOPHARYNGEAL_MET_VS_NON_DN	80	0.24	1.04	0.3846154	0.58551246
HSP27PATHWAY	15	0.36	1.04	0.42293233	0.59423953
4NQO_UNIQUE_FIBRO_UP	22	0.32	1.04	0.40789473	0.59475505
CASPASEPATHWAY	22	0.32	1.04	0.4198895	0.60099584
5FU_RESIST_GASTRIC_UP	21	0.33	1.03	0.39750445	0.60022527
BLEO_HUMAN_LYMPH_HIGH_24HRS_UP	92	0.24	1.03	0.38848922	0.6034646
MMS_HUMAN_LYMPH_HIGH_24HRS_UP	19	0.33	1.03	0.40459365	0.6063361
ET743PT650_COLONCA_DN	44	0.27	1.03	0.41064638	0.61773187
OLD_FIBRO_DN	147	0.21	1.02	0.4088586	0.6196439
NUMATA_G_CSF_DIFF	18	0.33	1.02	0.4163498	0.61879355
PARK_MSCS_DIFF	28	0.30	1.02	0.42446044	0.6254833
ELONGINA_KO_UP	146	0.21	1.02	0.40604028	0.6247075
ADIP_DIFF_UP	64	0.24	1.02	0.41996235	0.6241856
HDACI_COLON_SUL_DN	182	0.21	1.02	0.41254124	0.6243742
ROSS_MLL_FUSION	83	0.23	1.02	0.3979933	0.62325174
CIRCADIAN_EXERCISE	40	0.27	1.02	0.439781	0.6237854
STRESS_GENOTOXIC_SPECIFIC_DN	39	0.27	1.02	0.41165414	0.62488467
LEE_MYC_TGFA_UP	60	0.25	1.02	0.4293578	0.6281788
TPA_RESIST_MIDDLE_DN	107	0.23	1.02	0.41074523	0.62840784
NELSON_ANDROGEN_UP	59	0.25	1.02	0.43201378	0.62761223
WERNER_FIBRO_DN	153	0.21	1.01	0.4152824	0.6306369
FALT_BCLL_UP	44	0.27	1.01	0.43144423	0.63283724
TPA_RESIST_LATE_DN	63	0.24	1.01	0.4509804	0.63199824
AGUIRRE_PANCREAS_CHR1	31	0.28	1.01	0.4379845	0.6335119
G1PATHWAY	25	0.30	1.01	0.43486238	0.63261086
HOFMANN_MDS_CD34_LOW_RISK	50	0.26	1.01	0.44247788	0.6422029
TNFALPHA_30MIN_UP	40	0.27	1.01	0.41856393	0.6424858
COCAINE_BRAIN_4WKS_UP	55	0.25	1.01	0.45276293	0.6418017
ZMPSTE24_KO_DN	24	0.30	1.00	0.4364641	0.65185815
MEF2DPATHWAY	18	0.33	1.00	0.4331551	0.65169734
SA_CASPASE_CASCADE	16	0.34	1.00	0.4638219	0.65309066
FLECHNER_KIDNEY_TRANSPLANT_REJECTION_PBL_DN	51	0.25	1.00	0.48677248	0.6542953
DAC_BLADDER_UP	28	0.29	1.00	0.4524237	0.65954536
ZHAN_MMPC_EARLYVS	48	0.25	1.00	0.4651163	0.6594456
UVC_LOW_ALL_UP	19	0.32	0.99	0.4610895	0.66444093
FLOTHO_CASP8AP2_MRD_DIFF	84	0.23	0.99	0.49464285	0.66635865
AGUIRRE_PANCREAS_CHR9	24	0.30	0.99	0.478424	0.66979384
PENG_LEUCINE_UP	102	0.22	0.99	0.4832776	0.67257965
AGEING_KIDNEY_SPECIFIC_UP	147	0.21	0.99	0.4825784	0.674935
FSH_GRANULOSA_UP	78	0.23	0.99	0.48448277	0.67743576
OXSTRESS_RPETHREE_DN	28	0.28	0.98	0.5	0.6814511
MARCINIAK_CHOP_DIFF	19	0.31	0.98	0.47519085	0.6874091
NF90_DN	38	0.26	0.98	0.49183303	0.6949148
AGUIRRE_PANCREAS_CHR6	32	0.27	0.98	0.4990758	0.6941297
FRUCTOSE_AND_MANNOSE_METABOLISM	25	0.28	0.98	0.4682836	0.69407785
UVC_TTD_4HR_UP	58	0.24	0.97	0.52149534	0.7038413
HDACI_COLON_CLUSTER10	34	0.27	0.97	0.50774527	0.7063619
PASSERINI_APOPTOSIS	42	0.25	0.97	0.51526034	0.7108989
HSC_STHSC_SHARED	26	0.28	0.97	0.5061082	0.710461
ST_INTEGRIN_SIGNALING_PATHWAY	75	0.23	0.97	0.5254833	0.7122664
IDX_TSA_DN_CLUSTER1	41	0.26	0.97	0.5248227	0.71184313
FLECHNER_KIDNEY_TRANSPLANT_WELL_PBL_DN	42	0.26	0.96	0.5043029	0.71320784
HASLINGER_B_CLL_12	18	0.31	0.96	0.50961536	0.7166376
CALRES_MOUSE_NEOCORTEX_DN	63	0.23	0.96	0.5282332	0.7164273
IL1_CORNEA_DN	74	0.23	0.96	0.50431776	0.71574724
CALRES_MOUSE_UP	28	0.28	0.96	0.54442346	0.71847177
UNDERHILL_PROLIFERATION	16	0.33	0.96	0.51272017	0.7170491
HYPOXIA_FIBRO_UP	20	0.31	0.96	0.5222222	0.71863437
ADIPOGENESIS_HMSC_CLASS3_UP	60	0.23	0.96	0.5294118	0.71862584

VANASSE_BCL2_TARGETS	76	0.23	0.96	0.5357766	0.72072184
ATMPATHWAY	19	0.30	0.95	0.51361865	0.72621965
HDACI_COLON_CUR2HRS_UP	26	0.29	0.95	0.5092937	0.7299117
HDACI_COLON_BUT24HRS_UP	61	0.23	0.95	0.5265866	0.73011124
SMITH_HTERT_DN	61	0.23	0.95	0.5320285	0.72982943
HSC_STHSC_FETAL	26	0.28	0.95	0.5130597	0.7286313
ST_P38_MAPK_PATHWAY	35	0.26	0.95	0.5274102	0.73085004
DNMT1_KO_DN	15	0.32	0.95	0.53759396	0.72974217
FRASOR_ER_UP	30	0.27	0.95	0.5413534	0.7336032
PASSERINI_PROLIFERATION	63	0.23	0.95	0.5303571	0.7336205
CMV-UV_HCMV_6HRS_UP	120	0.20	0.95	0.57213116	0.7365311
UVB_NHEK1_C2	21	0.31	0.94	0.5420744	0.7362541
CERAMIDEPATHWAY	22	0.29	0.94	0.5343228	0.74027187
CMV_HCMV_TIMECOURSE_16HRS_DN	20	0.30	0.94	0.5212569	0.7444169
CHEN_HOXA5_TARGETS_UP	229	0.19	0.94	0.6175973	0.74416256
AGED_MOUSE_HIPPOCAMPUS_ANY_DN	39	0.26	0.94	0.5300353	0.7439857
IDX_TSA_UP_CLUSTER1	23	0.29	0.94	0.5553539	0.7433601
CMV_HCMV_TIMECOURSE_ALL_UP	462	0.17	0.94	0.65486723	0.74566585
ARGININE_AND_PROLINE_METABOLISM	41	0.25	0.94	0.53565216	0.7443315
STOSSI_ER_UP	47	0.24	0.94	0.5732369	0.7435975
LH_GRANULOSA_UP	80	0.22	0.94	0.60595447	0.7469236
STARCH_AND_SUCROSE_METABOLISM	31	0.26	0.93	0.56013745	0.7482369
LI_FETAL_VS_WT_KIDNEY_UP	179	0.19	0.93	0.63	0.75025284
NOUZOVA_CPG_METHLTD	49	0.24	0.93	0.5893186	0.7555817
CMV_HCMV_TIMECOURSE_24HRS_UP	72	0.22	0.92	0.63202727	0.787985
CMV_HCMV_TIMECOURSE_20HRS_UP	84	0.21	0.92	0.6077441	0.78850424
UVC_HIGH_ALL_DN	295	0.18	0.92	0.68611985	0.78800255
PARK_MSCS_LIN2	38	0.24	0.92	0.5970149	0.78792495
HSC_HSCANDPROGENITORS_SHARED	452	0.16	0.91	0.8032787	0.8070863
DFOSB_BRAIN_8WKS_UP	36	0.25	0.91	0.5919854	0.8073602
TPA_SENS_MIDDLE_DN	299	0.17	0.90	0.7488076	0.8133518
AGED_MOUSE_CORTEX_UP	31	0.25	0.90	0.61869156	0.8118585
BECKER_TAMOXIFEN_RESISTANT_UP	40	0.24	0.90	0.6258865	0.814276
HSC_HSCANDPROGENITORS_ADULT	459	0.17	0.90	0.81765556	0.8142199
NADLER_OBESITY_UP	50	0.23	0.90	0.64354527	0.81778145
HSC_STHSC_ADULT	30	0.26	0.90	0.60853434	0.8168978
CANCERDRUGS_PROBCELL_UP	15	0.30	0.90	0.5777778	0.81750727
FLECHNER_KIDNEY_TRANSPLANT_REJECTION_PBL_UP	64	0.22	0.90	0.6443662	0.8170918
STRESS_GENOTOXIC_SPECIFIC_UP	33	0.25	0.90	0.61759424	0.81671506
UREA_CYCLE_AND_METABOLISM_OF_AMINO_GROUPS	17	0.30	0.90	0.5896488	0.81583756
RADIATION_SENSITIVITY	24	0.27	0.90	0.6143667	0.8154305
RACCYCDPATHWAY	22	0.28	0.89	0.61690646	0.82110184
NEMETH_TNF_UP	77	0.21	0.89	0.7023593	0.82724553
HSC_HSCANDPROGENITORS_FETAL	452	0.16	0.89	0.8371758	0.8293209
UVC_TTD-XPCS_COMMON_UP	21	0.28	0.89	0.621881	0.830179
BRUNO_IL3_DN	63	0.21	0.89	0.654386	0.83065796
XU_ATRA_PLUSNSC_UP	15	0.30	0.88	0.61496353	0.8324343
PORPHYRIN_AND_CHLOROPHYLL_METABOLISM	20	0.27	0.88	0.61452514	0.8336124
HDACI_COLON_BUT16HRS_UP	35	0.25	0.88	0.64285713	0.83898336
ZHAN_TONSIL_PCBC	43	0.23	0.88	0.63925236	0.840703
ASTIER_BCELL	60	0.22	0.88	0.654321	0.84039044
WALKER_MM_SNP_DIFF	43	0.23	0.88	0.66608393	0.84196573
PASSERINI_OXIDATION	19	0.28	0.88	0.6455696	0.84118116
ADIP_VS_PREADIP_UP	35	0.24	0.88	0.6809269	0.84165937
JECHLINGER_EMT_UP	53	0.22	0.87	0.6857671	0.8449433
GRANDVAUX_IRF3_DN	20	0.27	0.87	0.64606744	0.8467824
ASTIER_FN_DIFF	61	0.21	0.87	0.70780396	0.851732
GALACTOSE_METABOLISM	23	0.27	0.87	0.6582524	0.85297567
LEE_E2F1_UP	60	0.21	0.87	0.6958763	0.85223955
CMV_HCMV_TIMECOURSE_6HRS_DN	52	0.22	0.87	0.704797	0.8547756
ST_JNK_MAPK_PATHWAY	40	0.23	0.86	0.6848816	0.864193
FSH_OVARY_MCV152_UP	61	0.21	0.86	0.72136754	0.868119
LEE_MYC_E2F1_DN	61	0.21	0.85	0.72035396	0.87604517
SHEPARD_POS_REG_OF_CELL_PROLIFERATION	88	0.19	0.85	0.7752809	0.8745889

YAGI_AML_PROG_ASSOC	125	0.18	0.85	0.79401994	0.88328975
UEDA_MOUSE_SCN	74	0.20	0.84	0.7465278	0.8937752
HDACI_COLON_TSA_UP	100	0.19	0.84	0.8016667	0.8956394
BRCA1KO_MEF_DN	77	0.19	0.84	0.77208483	0.902276
KNUDSEN_PMNS_DN	225	0.16	0.84	0.8998358	0.9035818
UVC_TTD_ALL_UP	76	0.20	0.84	0.7849829	0.90385085
NITROGEN_METABOLISM	21	0.26	0.83	0.7106691	0.9076688
UV-CMV_UNIQUE_HCMV_6HRS_UP	102	0.19	0.83	0.80762565	0.9084662
CORDERO_KRAS_KD_VS_CONTROL_DN	55	0.21	0.83	0.7531306	0.90741503
HYPERTROPHY_MODEL	20	0.26	0.83	0.69475657	0.90862465
GH_GHRHR_KO_24HRS_UP	115	0.18	0.83	0.8158784	0.90964115
APOPTOSIS_GENMAPP	43	0.22	0.83	0.75768536	0.9154663
WELCSH_BRCA_UP	38	0.22	0.82	0.75938565	0.91955125
HIVNEFPATHWAY	55	0.21	0.82	0.76094276	0.92016625
UCALPAINPATHWAY	15	0.29	0.82	0.71666664	0.9188358
CPR_NULL_LIVER_DN	16	0.27	0.82	0.7368421	0.91757196
KUROKAWA_5FU_IFN_SENSITIVE_VS_RESISTANT_DN	31	0.24	0.82	0.74285716	0.91899
CIS_RESIST_GASTRIC_UP	16	0.28	0.82	0.7137331	0.91903114
ZHAN_MM_CD1_VS_CD2_UP	69	0.19	0.82	0.81607145	0.9179402
AGED_MOUSE_MUSCLE_DN	31	0.23	0.82	0.7679856	0.9165981
PARK_HSC_VS_MPP_UP	16	0.27	0.82	0.71789885	0.91866
GUO_HEX_DN	54	0.20	0.82	0.7927273	0.9181485
STEMCELL_COMMON_DN	55	0.21	0.81	0.7714286	0.91935587
KANNAN_P53_UP	35	0.22	0.81	0.7807183	0.9258394
POMEROY_DESMOPLASIC_VS_CLASSIC_MD_UP	46	0.21	0.81	0.827957	0.9258542
MCALPAINPATHWAY	22	0.25	0.80	0.75438595	0.9353035
PASSERINI_EM	34	0.22	0.79	0.7973231	0.94865847
RETT_UP	28	0.23	0.79	0.8238342	0.9483066
HDACI_COLON_CUR_DN	38	0.21	0.79	0.8074074	0.94794625
TPA_SENS_MIDDLE_UP	65	0.19	0.79	0.8398637	0.9485715
BCL2_FAMILY_AND_REG_NETWORK	21	0.25	0.79	0.7429643	0.9475947
ROSS_CBF_LEUKEMIA	65	0.19	0.79	0.8288288	0.9469906
FETAL_LIVER_ENRICHED_TRANSCRIPTION_FACTORS	75	0.18	0.79	0.8563734	0.94782406
INSULIN_NIH3T3_UP	16	0.27	0.79	0.7606679	0.9483416
WNT_SIGNALING	58	0.19	0.78	0.8438061	0.9528483
VANTVEER_BREAST_OUTCOME_GOOD_VS_POOR_UP	25	0.23	0.78	0.78142077	0.95372117
IDX_TSA_DN_CLUSTER2	56	0.19	0.78	0.85910654	0.9527677
GLYCEROLIPID_METABOLISM	40	0.21	0.78	0.8203704	0.956654
PARK_MSCS_BOTH	41	0.21	0.78	0.8318584	0.9566513
MAPKPATHWAY	84	0.18	0.78	0.8896926	0.95607436
UVC_LOW_C3_DN	19	0.25	0.78	0.80263156	0.9548353
HDACI_COLON_BUT12HRS_UP	38	0.21	0.78	0.8131868	0.9543566
CMV_HCMV_TIMECOURSE_4HRS_DN	35	0.21	0.77	0.83773583	0.9560878
POMEROY_MD_TREATMENT_GOOD_VS_POOR_UP	29	0.22	0.77	0.8068834	0.9584538
NICK_RHAPC_UP	32	0.22	0.77	0.83733827	0.96007544
CIS_XPC_DN	182	0.16	0.77	0.96135265	0.95964104
AGEING_LYMPH_DN	17	0.26	0.77	0.7858509	0.9594571
STEFFEN_AML_PML_PLZF_TRGT	42	0.20	0.76	0.856102	0.96229863
NAKAJIMA_MCSMBP_EOS	27	0.23	0.76	0.8244275	0.9610208
WERNERONLY_FIBRO_DN	53	0.19	0.76	0.8627787	0.95965964
CMV_HCMV_TIMECOURSE_16HRS_UP	56	0.19	0.76	0.86762077	0.95886266
UVC_XPCS_8HR_DN	408	0.14	0.76	0.99375975	0.9630641
AKTPATHWAY	17	0.25	0.76	0.8038095	0.96435684
TOLLPATHWAY	30	0.22	0.75	0.8611111	0.96675205
P53PATHWAY	16	0.25	0.75	0.81620556	0.966609
WANG_HOXA9_VS_MEIS1_UP	24	0.23	0.75	0.85634327	0.9658775
CMV_HCMV_TIMECOURSE_8HRS_UP	20	0.24	0.75	0.81906617	0.96633947
CREB_BRAIN_8WKS_DN	44	0.20	0.75	0.87456447	0.9654578
ROSS_CBF	82	0.17	0.75	0.9189655	0.96586585
NADLER_OBESITY_HYPERGLYCEMIA	42	0.20	0.74	0.887522	0.9726879
IFN_BETA_GLIOMA_UP	61	0.18	0.73	0.9274336	0.98141354
INTEGRINPATHWAY	32	0.21	0.73	0.89700377	0.98095673
UVC_XPCS_ALL_DN	478	0.13	0.73	0.99852943	0.9807129
UVB_NHEK3_C5	35	0.20	0.72	0.8686679	0.98764163

VIPPATHWAY	25	0.22	0.72	0.8950382	0.98809266
CALRES_RHESUS_DN	59	0.18	0.72	0.9348659	0.9867763
GH_GHRHR_KO_6HRS_UP	62	0.17	0.72	0.9480069	0.9856163
GLYCOGEN_METABOLISM	33	0.20	0.72	0.8821363	0.98469573
DISTECHE_XINACTIVATED_GENES	19	0.23	0.71	0.8735849	0.985489
GLYCINE_SERINE_AND_THREONINE_METABOLISM	32	0.20	0.71	0.8817204	0.98527503
P53GENES_ALL	17	0.24	0.71	0.85528755	0.9892081
FERRARI_4HPR_UP	22	0.22	0.71	0.86972475	0.9889545
HALMOS_CEBP_UP	50	0.18	0.70	0.92375886	0.9884016
OLDWERNER_FIBRO_UP	21	0.22	0.70	0.89694655	0.98823684
WELCH_GATA1	24	0.21	0.70	0.89444447	0.98797274
SARCOMAS_LEIOMYOSARCOMA_CALP_UP	15	0.24	0.69	0.8676749	0.99199724
MPRPATHWAY	22	0.21	0.69	0.89048475	0.99051875
UVC_TTD-XPCS_COMMON_DN	144	0.14	0.69	0.9829932	0.99610823
FALT_BCLL_IG_MUTATED_VS_WT_DN	48	0.17	0.68	0.94332725	0.9955903
OLDONLY_FIBRO_DN	46	0.18	0.68	0.9488536	0.9957143
IRS_KO_ADIP_UP	23	0.20	0.68	0.9171375	0.9980726
IDX_TSA_DN_CLUSTER6	19	0.22	0.68	0.9005736	0.9965676
UVC_HIGH_D4_DN	46	0.17	0.67	0.9580292	1
PASSERINI_ADHESION	36	0.18	0.66	0.94332725	1
LIZUKA_L0_GR_L1	15	0.23	0.66	0.89325845	1
LIAN_MYELOID_DIFF_TF	34	0.18	0.65	0.945591	1
HDACI_COLON_TSA48HRS_UP	35	0.18	0.65	0.9508772	1
UVC_LOW_ALL_DN	58	0.16	0.65	0.98317754	1
HDACI_COLON_SUL12HRS_DN	22	0.20	0.64	0.93670887	1
HDACI_COLON_TSA2HRS_UP	49	0.16	0.64	0.9655172	1
HDACI_COLON_BUT2HRS_UP	64	0.15	0.64	0.9882353	1
WONG_IFNA_HCC_RESISTANT_VS_SENSITIVE_UP	15	0.22	0.64	0.9209486	1
OXSTRESS_RPE_H2O2TBH_DN	31	0.18	0.64	0.9507042	1
AS3_FIBRO_C1	31	0.18	0.64	0.96283185	1
WERNERONLY_FIBRO_UP	27	0.19	0.63	0.94280446	1
GLYCOSPHINGOLIPID_METABOLISM	22	0.20	0.63	0.9367311	1
CAMPTOTHECIN_PROBCELL_UP	17	0.21	0.63	0.9324578	1
STAEGE_EFTS_UP	21	0.20	0.63	0.93705034	0.9991407
WERNER_FIBRO_UP	48	0.16	0.63	0.9739777	0.99898016
AS3_FIBRO_C2	31	0.18	0.62	0.96103895	0.99906087
CMV_HCMV_TIMECOURSE_18HRS_UP	74	0.15	0.62	0.9907579	0.9988134
DORSAM_HOXA9_DN	30	0.18	0.62	0.96631205	0.9982026
HOFFMANN_BIVSBII_BI	88	0.14	0.61	0.99668324	0.99923736
DNMT1_KO_UP	70	0.15	0.61	0.9840142	0.99864036
ST_FAS_SIGNALING_PATHWAY	59	0.15	0.61	0.98734176	0.9973652
ACTINYPATHWAY	16	0.20	0.60	0.94382024	0.99725705
VERNELL_PRB_CLSTR2	20	0.19	0.60	0.9601518	0.99744314
S1P_SIGNALING	24	0.18	0.59	0.9671533	0.9961795
CITED1_KO_HET_DN	30	0.17	0.59	0.9711191	0.99565136
MMS_MOUSE_LYMPH_HIGH_24HRS_UP	22	0.19	0.59	0.9620939	0.9954256
TELPATHWAY	15	0.20	0.57	0.97445256	0.99743164
KENNY_WNT_DN	45	0.15	0.57	0.9944954	0.99697286
UV_UNIQUE_FIBRO_DN	30	0.15	0.52	0.9925373	1
ARFPATHWAY	15	0.18	0.52	0.985348	1
ZHAN_MM_CD1_VS_CD2_DN	42	0.14	0.51	1	1
ST_GA13_PATHWAY	35	0.14	0.49	0.9981818	0.99991035
HDACI_COLON_CUR24HRS_DN	17	0.16	0.49	0.99248123	0.99871933
ZHAN_MM_CD138_LB_VS_REST	24	0.15	0.48	0.9907749	0.9977673

Table S2. Comparison of the biological and clinical features of available MM mouse models

	Balb/c PCT[1]	5T2MM[2]	Bcl_{XL}xiMYC[3]	WT C57BL[2]	EμXBP1[4]	Vk*MYC	Human MM	SCID-hu[5]
Strain	Balb/c	C57BL/KaLwRiJ	C57BL/6 x 129SvJ	C57BL/6 & C57BL/KaLwRiJ	C57BL/6	C57BL/6	n.a.	SCID
Requires transplant	No	Yes	No	No	No	No	No	Yes
Immuno-competent	Yes	Yes	Yes	Yes	Yes	Yes	Yes	No
Location	EM	BM,EM	BM,EM	BM	BM,EM	BM	BM	BM
Indolent	-	-	-	+	+	+	+	+
SHM (median)	n.d.	2.50%[6]	<1%	2.50%[6]	No	3.4%	8.8%[6]	n.a.
Most common Ig isotype	IgA	IgG	IgG>IgM	IgG	IgM>>IgG	IgG	IgG	n.a.
Age-related M-spike	?Yes	n.a.	Yes	Yes 30%@50w	Yes? 30%@50w	Yes 80%@50w	Yes	n.a.
IgG [g/l]	?	>5	n.d.	3.2 @70w	?	15 @70w	>35	1
x control		>2x control	5-10x control	control	1.5x control	5x control	5x control	n.a.
Anemia	No	Yes	n.d.	No	n.d.	Yes	Yes	n.a.
Osteoporosis	No	rare	n.d.	rare?	n.d.	Yes	Yes	Yes
Lytic bone disease	rare	Yes[7]	Yes	0.5%	Yes	Yes	Yes	Yes
Kidney disease	n.d.	rare	n.d.	n.d.	Yes	Yes	Yes	n.d.

n.a. Not applicable; n.d. Not done;

1. Potter, M., Neoplastic development in plasma cells. Immunol Rev, 2003. **194**: p. 177-95.
2. Radl, J., et al., Animal model of human disease. Multiple myeloma. Am J Pathol, 1988. **132**(3): p. 593-7.
3. Cheung, W.C., et al., Novel targeted deregulation of c-Myc cooperates with Bcl-X(L) to cause plasma cell neoplasms in mice. J Clin Invest, 2004. **113**(12): p. 1763-73.
4. Carrasco, D.R., et al., The differentiation and stress response factor XBP-1 drives multiple myeloma pathogenesis. Cancer Cell, 2007. **11**(4): p. 349-60.
5. Yaccoby, S., B. Barlogie, and J. Epstein, Primary myeloma cells growing in SCID-hu mice: a model for studying the biology and treatment of myeloma and its manifestations. Blood, 1998. **92**(8): p. 2908-13.
6. Zhu, D., et al., Immunoglobulin VH gene sequence analysis of spontaneous murine immunoglobulin-secreting B-cell tumours with clinical features of human disease. Immunology, 1998. **93**(2): p. 162-70.
7. Vanderkerken, K., et al., Follow-up of bone lesions in an experimental multiple myeloma mouse model: description of an in vivo technique using radiography dedicated for mammography. Br J Cancer, 1996. **73**(12): p. 1463-5.